

## SIMULATION ANALYSIS OF DOUBLY FED INDUCTION GENERATOR FOR WIND ENERGY CONVERSION SYSTEM USING MATLAB

H. M. B. Metwally, M. A. Farahat, and M. A. Sadek

*Electrical Power Engineering Department, Faculty of Engineering,  
Zagazig University, Zagazig, EGYPT*

### ABSTRACT

The doubly fed induction generator (DFIG), used as a wind turbine generator, has recently received a great attention from the industrial and scientific communities. The reasons of that are: it easily produces a fixed frequency from the stator windings when the rotor is driven at variable speed, and the excitation power electronic converter feeding the rotor windings needs to be rated at a fraction of the nominal power of the generator. The aim of this paper is to develop a mathematical model for the Wind Energy Conversion system (WEC) driving a DFIG. The steady-state simulation model of the DFIG is developed using MATLAB. Simulation analysis is performed to investigate the DFIG characteristics including torque, real power and reactive power with speed (i.e. slip) characteristics. Comparison with measured characteristics shows a close agreement which indicates that the model is accurate.

لقد نال المولد الحثي ثنائي التغذية إهتماما كبيرا في الأوساط العلمية والصناعية في الآونة الأخيرة لإستخدامه كمولد كهربي مع نظم التربينات الهوائية وذلك للأسباب الآتية , أولا لأن القوة الدافعة الكهربية المتولدة تكون ثابتة التردد مهما كانت سرعة المولد وثانيا لأن القدرة الكهربية المطلوبة لتغذية دائرة العضو الدوار تكون صغيرة جدا بالمقارنة بالقدرة الكهربية للمولد مما يقلل جدا من تكاليف دائرة القدرة الإلكترونية المطلوبة. في هذا البحث تم تطوير نموذج رياضي لتربينه هوائية تحرك مولد حثي ثنائي التغذية وتم تطوير برنامج محاكاة لدراسة خواص المولد في حالة الإستقرار وذلك بالإستعانة ببرنامج الماتلاب , وتشمل هذه الخواص كيفية تغير العزم والقدرة الفعالة والقدرة الغير فعالة مع تغير السرعة , ولقد ثبت أن النتائج النظرية التي تم الحصول عليها من البرنامج تتطابق مع النتائج العملية مما يؤكد دقة النموذج الرياضي الذي تم تطويره.

### 1. INTRODUCTION

As a result of increasing environmental concern, it is required to minimize the impact of conventional electricity generation on the environment. Therefore efforts are made to generate electricity from renewable sources. One way of generating electrical energy from renewable sources is to use electricity wind turbines that convert the energy contained in the flowing air. Several types of Wind Turbine (WT) systems are now available and are in use: fixed speed WT drives a squirrel cage induction generator (SCIG) with limited speed range variation ( $\pm 2\%$ ) is an example. The advantages of this system are simplicity, reduced unit cost, brushless and low maintenance [1].

WT drives an Opti-slip induction generator with limited speed range variation ( $\pm 10\%$ ) is also in use. It consists of wound rotor induction generator (WRIG) with scalar rotor current control by adding external resistance in the rotor circuit. In this type the slip of the generator is changed by modifying the total rotor resistance by means of a converter

mounted on the rotor shaft as in Fig. 1. The converter is optically controlled, which means that no slip rings are necessary, this type reduces the mechanical loads and power fluctuations caused by gusts as the difference between the turbine torque and controlled generator torque decreases [2]; The disadvantages are limited speed rang (only  $\pm 10\%$ ), requirement of reactive power compensation system and high rotor losses which increase the temperature of the generator winding.

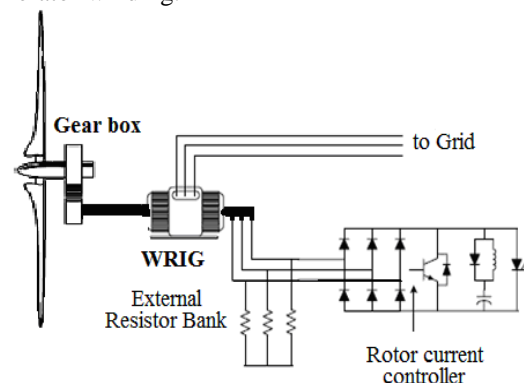


Fig. 1 WT drives an Opti-slip induction generator

There is also another type of WT generators as full scale variable speed WT driving a (SCIG or wound rotor synchronous generator, or permanent magnet synchronous generator) with fully rated converter to convert the generated frequency to the grid frequency. These types with fully rated converters are not used in Egypt till now.

The famous WT generator is the DFIG which consists of a WRIG with stator windings directly connected to the constant frequency grid and rotor windings connected to a bidirectional back-to-back IGBT voltage source converter as shown in Fig. 2. This system allows a variable speed operation over a large, but restricted range ( $\pm 30\%$ ).

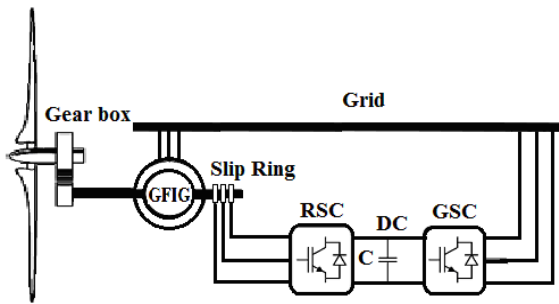


Fig. 2 DFIG wind turbine system

Recently, the WT with DFIG is becoming popular because it has the characteristics of high energy transfer efficiency, low investment, flexible control, and the converters only supply the exciting current of DFIG rotor. Hence its capacity is fairly low; approximately (20-25%) of the DFIG rated capacity [3].

## 2. MODELING OF WIND TURBINE SYSTEM

### 2.1 Wind Speed Model

Wind power is the power input to wind power generation system. The wind velocity usually varies, as shown in Fig. 3, and has a stochastic character. The wind speed is modeled as [4]

$$v(t) = v_0 \left[ 1 + \sum_k A_k \sin(\omega_k t) \right] + \frac{2V_{gmax}}{1 + e^{-4(\sin(\omega_g t) - 1)}} \quad (1)$$

Where  $v_0$  is the average value of wind velocity in (m/sec),  $A_k$  is the amplitude of  $K_{th}$  harmonic,  $\omega_k$  is the frequency of  $K_{th}$  harmonic,  $V_{gmax}$  is the gust amplitude and  $\omega_g$  is the gust frequency. Figure 3, shows wind speed variation for four hour in Zafarana wind farm, in Egypt, the largest site in the Middle East.

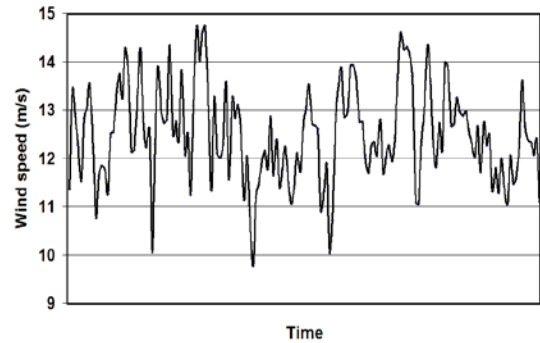


Fig. 3 Wind speed variation in Zafarana wind farm [5]

### 2.2 Wind Turbine Model

The available power in the wind is given by:

$$P_{wind} = \frac{1}{2} \rho A V^3 \quad (2)$$

Where:

$\rho$ : is the air density ( $= 1.225 \text{ Kg/m}^3$  at the sea level),  $A$ : is turbine swept area ( $\text{m}^2$ ),  
 $V$ : is the wind speed (m/sec.)

The mechanical power extracted from the wind ( $P_{mech}$ ) can be expressed as [6, 7]

$$P_{mech} = C_p P_{wind} \quad (3)$$

From equations (2) and (3):

$$P_{mech} = \frac{1}{2} \rho A V^3 C_p(\lambda, \beta) \quad (4)$$

Where:  $C_p$  is the power coefficient or the conversion efficiency of the turbine, each turbine has its own specific  $C_p$  and we can obtain its form as in reference [8]

$$C_p(\lambda, \beta) = 0.22 \left( \frac{116}{\lambda_i} - 0.4\beta - 5 \right) * e^{-\frac{22.5}{\lambda_i}} \quad (5)$$

$$\frac{1}{\lambda_i} = \frac{1}{\lambda + 0.08\beta} - \frac{0.035}{\beta^3 + 1} \quad (6)$$

Where

From equation 5 and 6 we can draw power coefficient ( $C_p$ ) vs. tip speed ratio ( $\lambda$ ) at constant pitch angle ( $\beta$ ) as shown in Fig. 4.

$\lambda$ : is the tip speed ratio, and it is given by

$$\lambda = \frac{\omega_r \cdot R}{V} \quad (7)$$

$\beta$ : is the blade pitch angle (degree),

$R$ : is the rotor radius (m)

$\omega_r$ : is the mechanical angular velocity of the turbine rotor in (rad/sec)

The mechanical torque or the aerodynamic torque (Tr) [9], from equations (4) and (7)

$$T_r = \frac{P_{mech}}{\omega_r} = \frac{1}{2} A \rho \frac{\omega_r^2 R^3}{\lambda^3} C_p(\lambda, \beta) \quad (8)$$

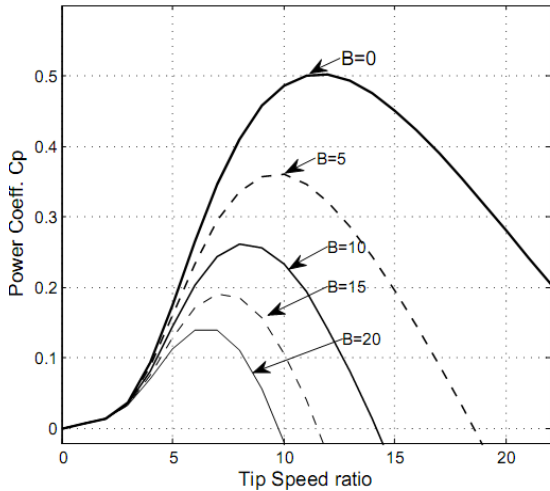


Fig. 4 Power coefficient vs. tip speed ratio at constant pitch angle

### 2.3 Drive Train Model

The drive train of wind turbine consists of blades, hub and low speed shaft, gearbox and high speed shaft (rotor of the generator). The following is the drive train model of the WTG system which is usually used in the power system analysis:

- **One-Mass Lumped Model**

In the one-mass or lumped model, all types of windmill drive train components are lumped together and work as a single rotating mass [10], as shown in Fig. 5.

All rotating masses are represented by one element, called 'lumped-mass' representation. The behavior can be expressed by the following differential equation:

$$J_T \dot{\omega}_r = T_r - K_T \omega_r - T_g \quad (9)$$

Where:  $J_T$  is the total rotating mass moment of inertia of the WT (N.m/(rad/sec<sup>2</sup>))

$T_g$ : Generator torque in the rotor side (N .m)

$K_T$ : Total external damping coefficient (N.m/(rad/sec))

### 2.4 Modeling of the Doubly Fed Induction Generator (DFIG)

The steady state electrical model of the DFIG is based on the single phase equivalent circuit for the doubly fed induction machine (DFIM) as shown in

Fig. 6 (a) with  $V_s$  being the rotor injected voltage [11]. The rotor resistance and the injected voltage can be divided into fixed value and a variable value. The fixed values represent the actual rotor resistance  $R_2$  and the actual injected voltage  $V_s$  while the variable terms represent the mechanical power. After simplification the equivalent circuit becomes as shown in Fig. 6 (b)

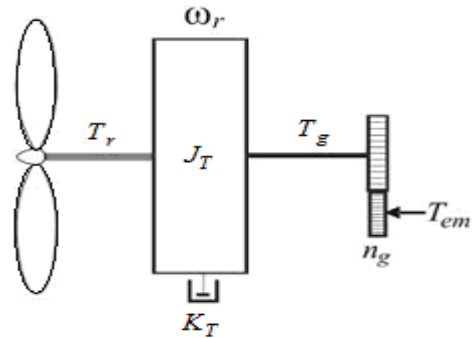


Fig. 5 Schematic diagram for One-mass drive train

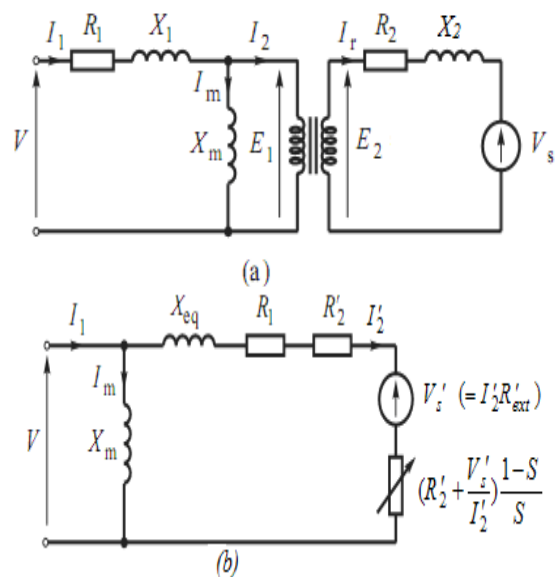


Fig. 6 Equivalent circuit of the DFIG

The injected rotor voltage  $V_s$  may be in phase with the rotor current  $I_2$  or out of phase with the rotor current  $I_2$ . For simplicity assume that  $V_s$  is in phase with the rotor current  $I_2$ ; This is equivalent to adding an external resistance  $R'_{ext} = V'_s / I'_s$ , equal to the ratio of the injected voltage to the rotor current, into the rotor circuit. Analysis of the simplified circuit of Fig. 6 (b) gives

$$I'_2 = \frac{V}{\sqrt{[R_1 + (R'_2 + \frac{V'_s}{I'_s}) \frac{1-s}{s}]^2 + X_{eq}^2}} \quad (10)$$

The total mechanical power of the DFIG is

$$P_{mech} = 3I_2'^2 (R_2' + \frac{V_s'}{I_2'}) \frac{1-S}{S}$$

(11) The mechanical torque of the DFIG can be obtained as:

$$T_{mech} = \frac{P_{mech}}{\omega_s (1-S)} \tag{12}$$

$$T_{mech} = \frac{3}{\omega_s} \frac{V^2}{[R_1 + (R_2' + \frac{V_s'}{I_2'}) \frac{1}{S}]^2 + X_{eq}^2} (R_2' + \frac{V_s'}{I_2'}) \frac{1}{S} \tag{13}$$

Where:

$\omega_s$  is the angular synchronous speed (rad/sec)

Rearranging the rotor current equation we can obtain:

$$S = \frac{I_2' R_2' + V_s'}{\sqrt{V^2 - [I_2' (X_{eq})]^2} - I_2' R_1} \tag{14}$$

At no load  $I_2' = 0$  and hence the slip equation reduces to

$$S_0 = \frac{V_s'}{V} \tag{15}$$

and the machine operates with a slip that depends on the magnitude and polarity of the injected voltage  $V_s$  as:

$V_s$ : Positive, slip becomes positive and the speed reduces: Sub-synchronous operation.

$V_s$ : Negative, slip becomes negative and the speed increases: Over-synchronous operation.

The positive value of  $V_s$  means the power is fed to the rotor and the negative value means the power is fed to the grid, and hence operation over a wide speed range both above and below synchronous speed is now possible by controlling the magnitude and polarity of the injected voltage.

### 2.5 Model of the Doubly Fed Converters

A doubly fed converter typically consists of back-to-back insulated gate bipolar transistor (IGBT) bridges coupled by a DC link as in Fig. 7. A DFIG control is usually divided into rotor and grid side controls, RSC and GSC respectively.

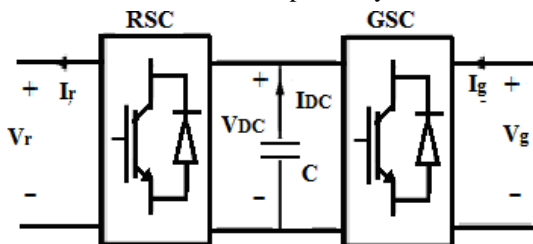


Fig. 7 Schematic diagram for doubly fed converter for DFIG

The rotor side converter (RSC) controls the power flow from the DFIG to the grid by controlling the rotor currents. The Grid Side Converter (GSC) ensures the regulation of the DC voltage to the desired value, in order to guarantee that the generated active power is fed via the DC-link to the grid.

Assuming a lossless converter [8, 12], the power balance equation is:

$$P_r = P_g + P_{DC} \tag{16}$$

Where:  $P_r$  is the power at the RSC (Watt)

$P_g$  : is the power at the GSC (Watt)

$P_{DC}$  : is the power dissipated in the DC-link (Watt), and is given by

$$P_{DC} = V_{DC} i_{DC} = CV_{DC} \frac{dV_{DC}}{dt} \tag{17}$$

### 3. CHARACTERISTICS OF THE DOUBLY FED INDUCTION GENERATOR

Using the mathematical model of the WT explained above, a simulation program based on MATLAB package is developed to predict the well known performance of the system. An effective way to study the operating conditions of a DFIG is to investigate its characteristic curves. The operating speed or slip of a DFIG is affected not only by wind speed but also by the injected rotor voltage, thus the turbine output power and electromagnetic torque characteristics of DFIG are different from traditional fixed speed induction generator used for wind power generation. Typical characteristic curves of a DFIG are torque, real power and reactive power versus speed characteristics. The data of the DFIG used in this paper is given in Table 1.

Table 1, The DFIG data used in the MATLAB simulation study [13]

Parameter	Value	Units
kVA (rated)	860	kW
Voltage (rated) V	690	V
I Current (rated)	721	A
Z base	0.957	$\Omega$
$R_1$	0.003469	p.u.
$X_1$	0.02651	p.u.
$R_2'$	0.002905	p.u.
$X_2'$	0.03691	p.u.
$X_m$	2.10379	p.u.
Frequency	50	Hz

**Case 1: Torque-speed characteristics at ( $V_d = 0$  p.u.) and variable  $V_q$  (0 to 0.2)**

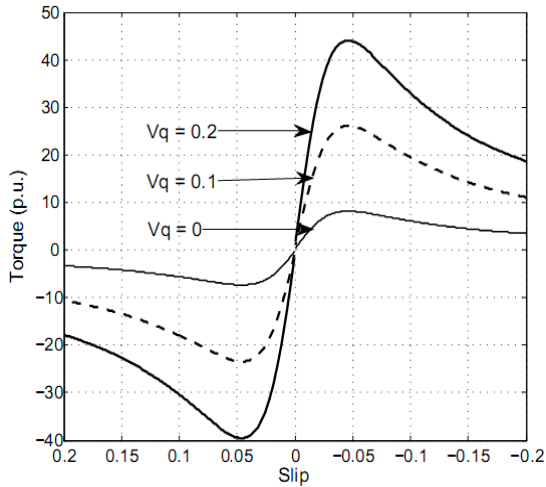


**Fig. 8** Simulated torque-speed characteristics at ( $V_d = 0$  p.u.)

The DFIG torque-speed characteristics are shown in Fig. 8, the imaginary component  $V_q$  of the injected rotor voltage changes from (0 to 0.2 p.u.) and the real component  $V_d$  is fixed at (0 p.u.). It can be seen that when both components of  $V_s$  are 0, the DFIG torque-speed characteristic is the same as that of the traditional induction generator. When increasing  $V_q$ , while keeping  $V_d$  at 0 p.u., the DFIG becomes more stable because the maximum torque increases.

**Case 2: Torque-speed characteristics at ( $V_q = 0.2$  p.u.) and variable  $V_d$**

The change of the real component  $V_d$  affects the DFIG torque characteristics. Figure 9 shows the DFIG torque-speed characteristics as  $V_d$  changes from (-0.2 p.u. to 0.2 p.u.) while  $V_q$  is fixed at 0.2 p.u.. With the increase of  $V_d$  positively the DFIG torque expand more to sub-synchronous range for its stable generating mode, and the DFIG becomes more stable because the pushover torque increases.

DFIG torque-speed characteristics depend mainly on the amplitude of the rotor-injected voltage when both  $V_q$  and  $V_d$  are positive, which means that an increase of either  $V_q$  or  $V_d$  can result in the expansion of the DFIG torque characteristics. However, when  $V_d$  is negative, as shown in Fig. 9 under constant  $V_q$ , the DFIG torque speed characteristics for its generating mode shrink but lower than the curves when  $V_d$  is positive.

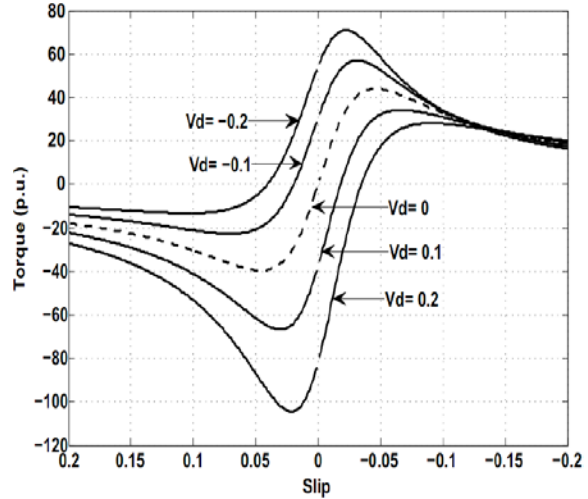


**Fig.9** Simulated torque speed characteristics ( $V_q = 0.2$ p.u.) and variable  $V_d$

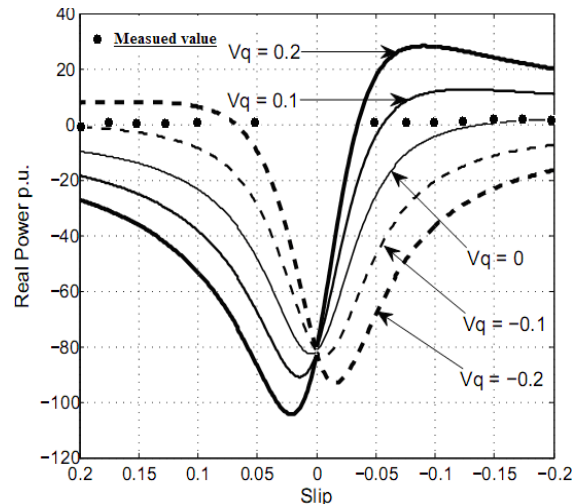


**Fig.10** Simulated DFIG real power- slip characteristics at  $V_d = 0.2$  p.u. and variable  $V_q$  with measured value plotted on it.

**Case 3: Real power characteristics at ( $V_d = 0.2$  p.u.) and variable  $V_q$**

The real power of DFIG is controlled by modifying  $V_q$  component of the injected rotor voltage. Figure 10 shows real power of the DFIG as  $V_q$  increases from -0.2 p.u. to 0.2 p.u. while  $V_d$  is kept constant at 0.2 p.u. From this figure, it can be concluded that, when  $V_q$  increases positively, the DFIG real power generation characteristics expanded more into sub- synchronous speed range and the generation pushover power of a DFIG rises too, showing enhanced DFIG stability and power generation capability. On the other hand, when either  $V_q$  increases negatively, the DFIG real power generation characteristics expanded more into over-synchronous speed range.

**Case 4: Reactive power characteristics at ( $V_q = 0.2$  p.u.) and variable  $V_d$**

In traditional induction machine, the machine takes inductive reactive power from the power supply system for its leakage and magnetizing reactive power needs. But, this situation is different for DFIG due to the injected rotor voltage. The reactive power of DFIG is controlled by modifying  $V_d$  component of the injected rotor voltage. Figure 11 shows the DFIG reactive power characteristics corresponding to  $V_q = 0.2$  and variable  $V_d$  (-0.2 to 0.2). The reactive power can be controlled in over-synchronous range by increasing  $V_d$  component positively, and can be controlled in sub-synchronous range by increasing  $V_d$  component negatively.

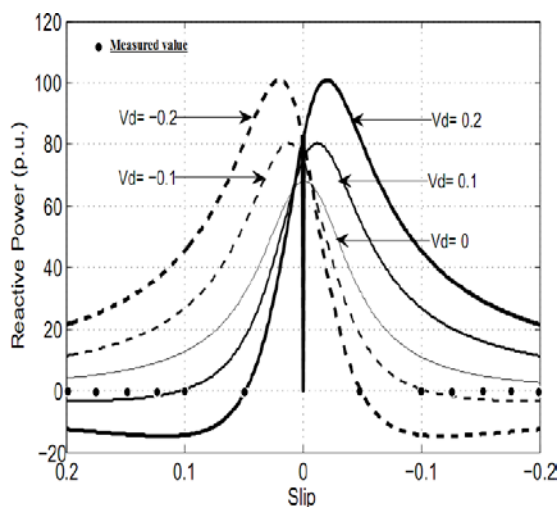


**Fig.11** Simulated DFIG reactive power characteristics at  $V_q = 0.2$  and variable  $V_d$  with measured value plotted on it.

**4. MEASURED CHARACTERISTICS FOR DFIG**

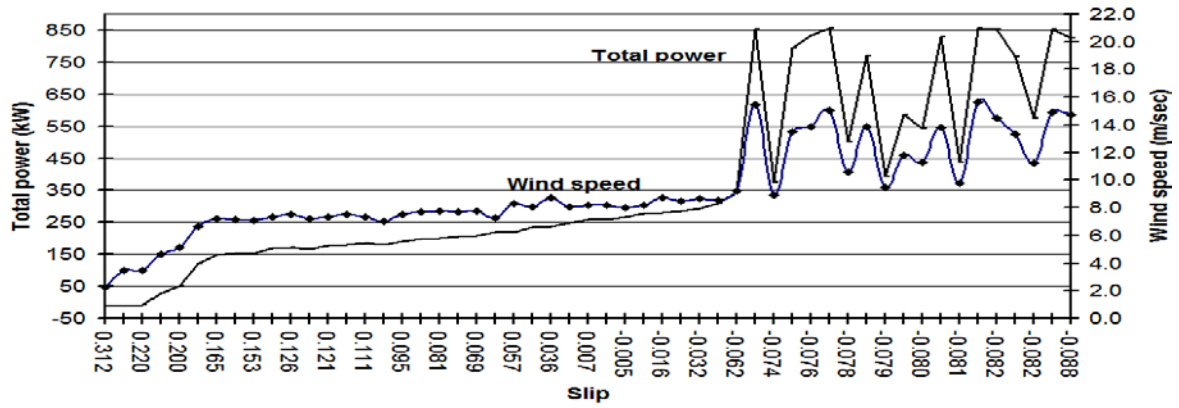
In this section, a practical data from Zafarana site is displayed. This data has been taken from online data program for the turbine of the case study [5]. Figure 12 shows the total power compared with wind speed, real stator and rotor power and reactive power versus the slip of the generator. The real power generated from the rotor circuit with its value positive or negative has been displayed. The negative value of the rotor power occurs with positive generator slip and this occurs at low wind speed (for this case at wind speed less than 8 m/sec). Figure 12(c) shows that the reactive power is absorbed from the grid by a little value and it doesn't exceed 10 kVAR and it goes to zero which mean the power factor is near unity without using capacitor bank, but actually it may be positive or negative depending on the operating conditions of the WT. The DFIG has the ability of reactive power control which means that the wind farm may be used for reactive power

correction of the network, and this option is used in some Europe countries like Spain for example [5]. From Figs. 10 and 11 comparisons between measured value and predicted value obtained from simulation analysis, the measured values is occurred and plotted in the stable region. The turbine controller has undefined number of curves to submit the desired values (active and reactive power) and each turbine have its own internal calculation for  $V_d$  and  $V_q$ . From Fig. 12, the rotor power has small value (positive or negative) not to exceed 50 kW, so the turbine actually operates at  $V_s$  under 0.1 p.u.. From Fig. 13, the measured real power is plotted on expanded simulated characteristics of real power ( at  $V_d = 0.2$  p.u. and  $V_q$  varies from 0.02 to 0.1 p.u.), the measured value submits the simulated curves, so we conclude that the predicted values are correct and can be obtained from DFIG and the modeling of the DFIG is valid.

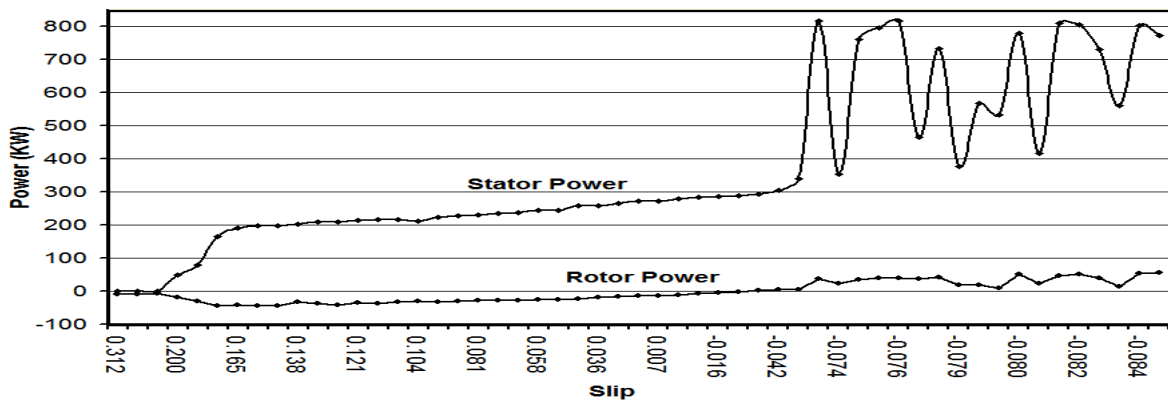
**5. CONCLUSION**

One of the most important modern wind turbines is the wind turbine equipped with DFIG with voltage source converter feeding the rotor circuit. The mathematical model of the wind turbine based on DFIG is developed. Then simulation program using the MATLAB package is developed, and used to predict the system characteristics at different operating conditions. Comparing the real time data with the simulation data we can conclude that the model of the system is accurate. Analyzing the results the following points are concluded:

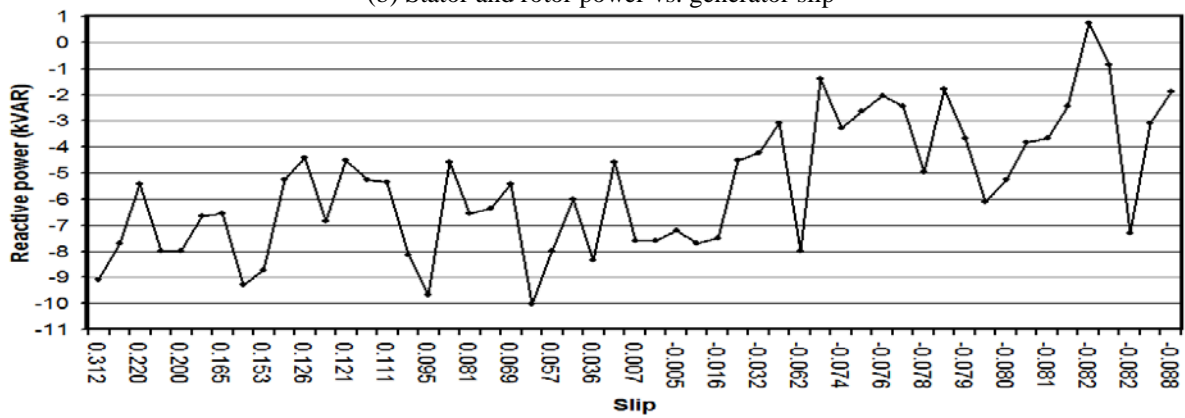
- Increasing the imaginary part of the rotor injected voltage ( $V_q$ ) increases the maximum torque and real power and the DFIG becomes more stable and the operating speed shifts to a sub-synchronous speed for its generating mode.
  - Increasing positively the real part of the rotor injected voltage ( $V_d$ ) for constant ( $V_q$ ), expands the DFIG torque and real power characteristics for its generating mode and reduces the inductive reactive power.
  - Increasing negatively the real part of the rotor injected voltage ( $V_d$ ) for constant ( $V_q$ ), shrinks the DFIG torque and real power characteristics for its generating mode and results in more inductive reactive power need.
- It can be concluded from the above analysis that optimal operation of DFIG in terms of torque, real power and reactive power requires proper control of injected rotor voltage  $V_s$ .



(a) Total power and wind speed vs. generator slip



(b) Stator and rotor power vs. generator slip



(c) Reactive power vs. generator slip

Fig.12 Measured value characteristics from Zafarana wind farm, Egypt [5].

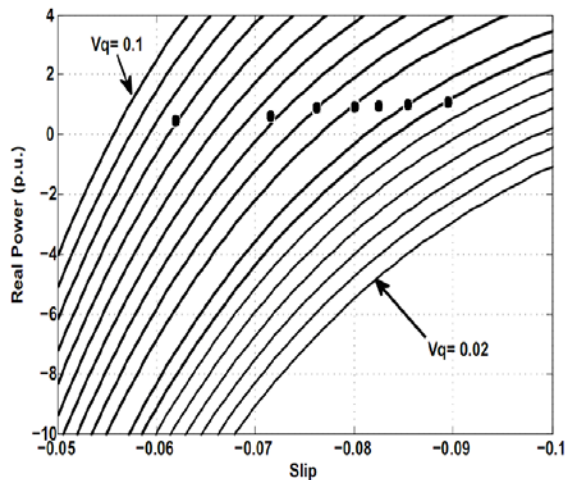


**Fig.13** Expanded simulated DFIG real power- slip characteristics at  $V_d = 0.2$  p.u. and variable  $V_q$  with measured value plotted on it

## 6. REFERENCES

- [1] Thomas Ackermann, "Wind Power in Power Systems", West Sussex, England: John Wiley & Sons, ISBN 0-470-85508-8, 2005.
- [2] D.J. Burnham, "Variable Rotor-Resistance Control of Wind Turbine Generators", Power & Energy Society General Meeting, PES '09, IEEE, 2009.
- [3] Feng Wu, Xiao-Ping Zhang, Keith Godfrey, and Ping Ju, "Modeling and Control of Wind Turbine with Doubly Fed Induction Generator", Power Systems Conference and Exposition, PSCE- IEEE -PES, pp: 1404 – 1409, IEEE, 2006.
- [4] Xing Zuoxial, Zheng Qionglin, Yao Xingjia, Jing Yanjun, "Integration of Large Doubly-fed Wind Power Generator System into Grid", Electrical Machines and Systems, ICEMS, Proceedings of the Eighth International Conference, IEEE, PP: 1000 – 1004, Vol. 2, 2005.
- [5] New and Renewable Energy Authority, Zafarana wind farm, Zafarana (7) project, SGIPE Program, 6th of July 2010.
- [6] Garlapati Satish Kumar, Avinash Kishore, "Dynamic Analysis and Control of Output Voltage of a Wind Turbine Driven Isolated Induction Generator", Industrial Technology, ICIT, IEEE International Conference, PP: 494 - 499, 2006.
- [7] J.G. Sloopweg, H. Polinder, W.L. Kling, "Dynamic Modelling of a Wind Turbine with Doubly Fed Induction Generator", Power Engineering Society Summer Meeting, IEEE, PP: 644 – 649, vol.1, 2001.
- [8] P. S. Mayurappriyan, Jovitha Jerome, M. Ramkumar, K. jambal, "Dynamic Modeling and Analysis of Wind Turbine Driven Doubly Fed Induction Generator", International Journal of Recent Trends in Engineering, Vol 2, No. 5, PP: 367-372, November 2009.
- [9] Xinfang ZHANG, Daping XU, Yibing LIU, "Intelligent control for large-scale variable speed variable pitch wind turbines", Journal of Control Theory and Applications, Volume 2, Number 3, PP: 305- 311, 2004.
- [10] Z. Mahi, C. Serban and H. Siguerdidjane, "Direct torque control of a doubly-fed induction generator of a variable speed wind turbine power regulation", Electric Power Components and Systems, Volume 30, Issue 2 , pages 199 – 216, France, 2007.
- [11] Jan Machowski, Janusz W. Bialek, James R. Bumby, "Power System Dynamics Stability and Control", Second Edition, John Wiley & Sons Ltd, ISBN: 978-0-470-72558-0, UK, 2008.
- [12] Xing-jia Yao, Lei Tian, Zuo-xia Xing and Xian-bin Su, "Dynamic Model and Simulation of Doubly Feed Induction Generator Wind Turbine", Automation and Logistics, ICAL '09', IEEE International Conference , PP: 1667 – 1671, 2009.
- [13] Doubly fed induction generator manual and start up, "NCR-450-L4/D – 850 KW", 28th of Jan, 2005.
- [14] Shuhui Li, Sitanshu Sinha, "A Simulation Analysis of Double-Fed Induction Generator for Wind Energy Conversion Using PSpice", IEEE Power Engineering Society General Meeting, ACTA Press, USA, 2006.
- [15] Muhammad H. Rashid, "Power Electronics: Circuit, Devices and applications", second edition, Prentice-Hall of India Private Limited, Sep. 1998.